

Electric polarization in a Chern insulator

Sinisa Coh and David Vanderbilt

Department of Physics & Astronomy, Rutgers University, Piscataway, NJ 08854-8019, USA
(Dated: February 20, 2024)

We extend the Berry-phase concept of polarization to insulators having a non-zero value of the Chern invariant. The generalization to such Chern insulators requires special care because of the partial occupation of chiral edge states. We show how the integrated bulk current arising from an adiabatic evolution can be related to a difference of bulk polarizations. We also show how the surface charge can be related to the bulk polarization, but only with a knowledge of the wavevector at which the occupancy of the edge state is discontinuous. Furthermore we present numerical calculations on a model Hamiltonian to provide additional support for our analytic arguments.

PACS numbers: 77.22.Ej; 73.43.-f; 73.20.At

In 1988 Haldane pointed out that an insulating crystal with broken time-reversal symmetry may exhibit a quantized Hall conductance even in the absence of a macroscopic magnetic field [1]. We shall refer to such a material as a "Chern insulator" (CI) because it necessarily would have a non-zero Chern invariant associated with its manifold of occupied Bloch states [2, 3]. While no CI has yet been discovered experimentally, there appears to be no reason why one could not exist, and theoretical models that behave as CIs are not difficult to construct. It seems plausible that the current blossoming of interest in exotic non-collinear magnets and multiferroics could yield an experimental example before long.

CIs occupy a middle ground between metals and ordinary insulators. Like metals, their conductivity tensor is non-zero, their surfaces are metallic (as a result of topological edge states crossing the Fermi energy), and it is impossible to construct exponentially localized Wannier functions (WFs) for them [4]. On the other hand, only the off-diagonal (dissipationless) elements of can be non-zero, the chiral edge states decay exponentially into the bulk, the one-particle density matrix decays exponentially in the interior [5], and the localization measure γ [6, 7] is finite [5] as in other insulators. Overall it appears natural to regard a CI as an unusual species of insulator, but many aspects of its behavior remain open to investigation.

As is well known, the electric polarization P is not well-defined in a metal. For an ordinary insulator, its definition alternatively in terms of Berry phases or WFs is by now well established [8, 9, 10]. For a CI, the absence of a Wannier representation removes the possibility of using it to define the polarization, and we shall show below that there is a fundamental difficulty with the Berry-phase definition as well. In view of the presence of dissipationless currents and metallic edge states, one might be tempted to conclude that P is not well-defined at all in a CI. On the other hand, γ is related to the fluctuations of P [11], and the finiteness of this quantity [5] suggests that the polarization might be well-defined after all.

The purpose of this Letter is to discuss whether, and

in what sense, a definition of electric polarization is possible in a CI. We demonstrate that the usual Berry-phase definition does remain viable if it is interpreted with care when connecting it to observables such as the internal current that flows in response to an adiabatic change of the crystal Hamiltonian, or to the surface charge at the edge of a bounded sample.

For the remainder of this Letter we restrict ourselves to the case of a 2D crystalline insulator having a single isolated occupied band. The generalization to the case of a 3D multiband insulator is not difficult, but would complicate the presentation. We also restrict ourselves to a single-particle Hamiltonian, noting that the principal difficulties in understanding CIs occur already at the one-particle level. The lattice vectors a_1 and a_2 are related to the reciprocal lattice vectors b_1 and b_2 in the usual way ($b_i \cdot a_j = 2\pi\delta_{ij}$) and the cell area is $S = |a_1 \times a_2|$.

The Berry-phase expression for the electric polarization can be written as

$$P_{[k_0]} = \frac{e}{(2\pi)^2} \text{Im} \int_{[k_0]} dk_1 \int_{[k_2]} dk_2 \mathbf{j}_k \cdot \mathbf{j}_{k_1} \quad (1)$$

where e is the charge quantum ($e > 0$), \mathbf{j}_k are the cell-periodic Bloch functions, and $[k_0]$ indicates the parallelogram reciprocal-space unit cell with origin at k_0 (that is, with vertices $k_0, k_0 + b_1, k_0 + b_1 + b_2$, and $k_0 + b_2$). In an ordinary insulator one insists on a smooth and periodic choice of gauge (relative phases of the \mathbf{j}_k) in Eq. (1), and P is well-defined (modulo $eR = S$, where R is a lattice vector [8]) independent of k_0 . However, in a CI such a gauge choice is no longer possible. To see this, we decompose $P_{[k_0]} = P_1 a_1 + P_2 a_2$, $k = k_1 b_1 + k_2 b_2$, and $k_0 = \alpha_1 b_1 + \alpha_2 b_2$, and rewrite Eq. (1) as

$$P_1^{[\alpha_2]} = \frac{e}{S} \int_{\alpha_1}^{\alpha_1+1} d\alpha_1 \int_{\alpha_2}^{\alpha_2+1} d\alpha_2 \frac{1}{2} \langle k_2 | \quad (2)$$

$$\gamma_1(k_2) = \text{Im} \int_{\alpha_1}^{\alpha_1+1} d\alpha_1 \int_{\alpha_2}^{\alpha_2+1} d\alpha_2 \mathbf{h}_{k_1, k_2} \cdot \mathbf{j}_{k_1} \mathbf{j}_{k_1 + k_2} \cdot \quad (3)$$

Eq. (3) is a Berry phase and is gauge independent modulo 2π (independent of α_1). This allows us to make an

arbitrary choice of branch for $\theta_1(k_2 = k_2)$ and to insist, as part of the definition of $P_1^{[2]}$, that $\theta_1(k_2)$ should remain continuous as k_2 is increased from k_2 to $k_2 + 1$. Since states at $(k_1; k_2)$ and $(k_1; k_2 + 1)$ are equivalent, it follows that

$$\theta_1(k_2 + 1) = \theta_1(k_2) + 2\pi C \quad (4)$$

where C is an integer. In fact C just defines the Chern number, and the insulator is a Chern insulator if $C \neq 0$. For simplicity we focus henceforth on a Chern insulator having $C = 1$.

Using Eqs. (2-3) and similar equations for P_2 , we have arrived at a definition $P_{[k_0]}$ that is well-defined, modulo eR/S as usual, even for a Chern insulator. However, as illustrated in Fig. 1(a),

$$P_{[k_0 + \hat{k}]} = P_{[k_0]} + \frac{eC}{2} \hat{z} \cdot \hat{k} \quad (5)$$

where \hat{z} is the unit vector along $a_1 \times a_2$. This dependence on k_0 clearly presents a problem for the interpretation of Eq. (2) as a "physical" polarization in the case of a Chern insulator.

However, let us recall how the concept of polarization is used. For a normal insulator at least [8], the change of polarization during an adiabatic change of some internal parameter of the system from time t_i to t_f is given by

$$\int_{t_i}^{t_f} dt J(t) = P_{[k_0]}^{(f)} - P_{[k_0]}^{(i)} \quad (\text{modulo } eR/S); \quad (6)$$

where $J(t)$ is the cell-averaged adiabatic current flowing in the bulk. A related statement, connected with the requirement that the charge pumped to the surface must be consistent with Eq. (6), is that the charge on an insulating surface normal to reciprocal vector b_1 is [9]

$$Q = P \cdot \hat{b}_1 \quad (\text{modulo } e/a_2); \quad (7)$$

Eqs. (6) and (7) embody the attributes of a useful definition of P . In the remainder of this Letter, we demonstrate that a generalized definition of P , having similar attributes, can be given in a Chern insulator. We first show that Eq. (6) remains correct, provided that the same k_0 (i.e., the same reciprocal-space cell) is used for $P^{(i)}$ and $P^{(f)}$ in Eq. (6). We also show that Eq. (7) must be modified and explain how. We provide numerical tests as well as analytic arguments for both claims.

We begin by giving two arguments for the correctness of Eq. (6) in the Chern insulator case. First, it is straightforward to see that the contribution to $J_1(t)$ can be computed independently for each k_2 [9], with the problem in $(k_1; t)$ space effectively corresponding to that of an ordinary 1D crystal. Thus, the derivation of Eq. (6) given in Ref. [8] goes through unchanged for the Chern insulator case. Second, we note that the expected result is obtained for the special case that the parameter of interest is a spatially uniform but time-dependent vector potential $A(t)$. Since a slow

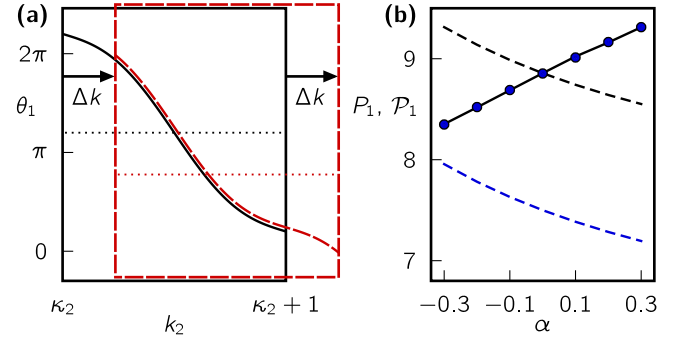


FIG. 1: (Color online) (a) Sketch of $\theta_1(k_2)$ in a Chern insulator ($C = +1$). Solid black and dashed red frames indicate reciprocal-cell origin chosen at k_2 and $k_2 + 1$ respectively. Dotted lines indicate corresponding averages, proportional to P_1 . (b) Computed $P_1(\alpha)$ and $P_1(\alpha)$ for the modified Haldane model, in units of $0.01e/S$, for adiabatic (dashed lines) and thermal (solid line and symbols) filling. See text.

tuning on of $A(t)$ causes state $u_k e^{ik \cdot r}$ to evolve into $u_{k + (e/c)A} e^{ik \cdot r}$, it follows that

$$P_{[k_0]}^{[A]} = P_{[k_0]}^{[A=0]} + \frac{e^2 C}{hc} \hat{z} \cdot A; \quad (8)$$

But a time-varying vector potential generates an electric field $E = (-1/c)dA/dt$, so that $J = (C\hbar/e)E$. The transverse conductivity σ_{xy} is thus quantized in units of e^2/h , expressing the fact that a Chern insulator is a realization of the integer quantum Hall effect [1].

We further confirm the validity of Eq. (6) by numerically testing our prediction on the Haldane model [1], a tight-binding model for spinless electrons on a honeycomb lattice at half filling with staggered site energies and complex second-neighbor hoppings chosen so that $C = 1$. Using the notation of Ref. [1], we adopt parameters $t_1 = 1$, $t_2 = 1 + 3\phi$, $\phi = -4$, $\phi = 2 + 3$ and the lattice vectors $a_1 = a_0(\sqrt{3}\hat{x} + \hat{y})/2$ and $a_2 = a_0\hat{y}$ (so that $a_1 \times a_2 = a_0^2\hat{z}$). Furthermore, we modify the first-neighbor hopping $t_1 \rightarrow t_1(1 + \phi)$ on the bonds parallel to $a_1 + a_2$ so as to break the threefold rotational symmetry and allow an adiabatic current to flow as ϕ is varied. The compensating ionic charge is assumed to sit on the site with lower site energy.

We consider an infinite strip of the Haldane model N_1 cells wide and extending to ∞ along y , as sketched in the inset of Fig. 2. States $u_{nk_2}(r)$ are labeled by k_2 , which remains a good quantum number, and an additional index $n = 1, \dots, 2N_1$. The dipole moment across the strip, per unit length, is

$$P_1 = \frac{e}{N_1 S} \int_0^{2\pi} dk_2 \sum_{n \in 2N_1(k_2)} \langle r_1 \rangle_{nk_2} \langle r_2 \rangle_{nk_2}; \quad (9)$$

where position vector r is decomposed as $r = r_1 a_1 + r_2 a_2$ and $N(k_2)$ is the set of occupied states to be discussed

shortly. In the limit of large N_1 , we associate the integrated current that flows along \hat{x} in the interior of the strip during an adiabatic evolution from $k_2 = k_2^i$ to $k_2 = k_2^f$ with the corresponding change in P_1 , since by continuity the charge must arrive at the surface. We then compare this with the change of P_1 evaluated using a single bulk unit cell via Eqs. (2-3) to validate the theory.

There is a subtlety, however. Neutrality implies that $N(k_2)$ contains N_1 states, but which ones? The problem arises because a CI is topologically required to have chiral metallic edge states. Our ribbon of CI therefore has one band of edge states along its left (L) edge and one along its right (R) edge (see inset of Fig. 2). For any given k_2 , let $k_2^*(k_2)$ be the value of k_2 at which L-edge and R-edge bands cross. A thermally induced filling of the edge states would correspond to the thick black curve for case k_2^i in Fig. 2, where the N_1 lowest-energy states are occupied at each k_2 and $k_2^f = k_2^*(k_2^i)$. Defining k_2^* to be the point at which the occupation switches between L and R edge states, we have $k_2^* = k_2^*$ for the thermalized case.

In general $k_2^*(k_2)$ varies with k_2 . However, k_2^* cannot change during an adiabatic evolution. Because we want to "measure" the polarization by the charge that accumulates at the surface, we specify that the adiabatic evolution is fast compared to the tunneling time between edge states but slow compared to all other processes, so that electrons cannot scatter between edges. Thus if we thermalize the system at k_2^i and then adiabatically carry the system from k_2^i to k_2^f , we arrive at the adiabatic filling illustrated by the thick red curve for case k_2^f in Fig. 2.

We thus expect that the change in polarization calculated from the right-hand side of Eq. (6) from the bulk bandstructure using Eqs. (1-3) should match that given by the change of Eq. (9) only if the adiabatic filling is maintained. We have confirmed this numerically for our modified Haldane model. The polarization as a function of k_2 calculated using Eq. (9) and using the right-hand side of Eq. (6) is indicated in Fig. 1(b) with black and blue dashed lines respectively [12]. Eqs. (2-3) were evaluated on a 300×300 k-point mesh. Eq. (9) was calculated using $N_1 = 25, 70$ and then extrapolating to infinity, while the k_2 integral was discretized with 5000 k-points. While there is a vertical offset between these curves that depends on the choice of k_0 in Eq. (6), the differences P_1 between different k_0 are correct at the level of 10^{-5} . On the other hand, the results obtained with the thermalized filling in Eq. (9), shown by the solid line in Fig. 1(b), are drastically different. These results confirm that the appropriate comparison is with the adiabatic filling, and provide numerical confirmation that Eq. (6) is indeed satisfied even in a CI.

We now turn to Eq. (7). A naive generalization to the CI case might be that $P_1 = P_{[k_0]} \hat{b}_1$ (modulo $e a_2$), but this cannot be correct. First, the left-hand side should be independent of k_0 , but the right-hand side is not. Second, the usual proof for ordinary insulators of the connection

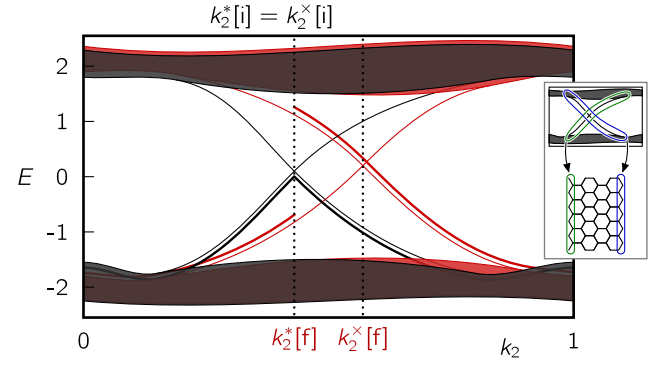


FIG. 2: (Color online) Sketch of a band structure of a finite ribbon of a Chern insulator. Solid regions indicate projected bulk bands; thin solid lines are edge states. Black and red correspond to k_2^i and k_2^f respectively; corresponding values of k_2 are indicated. Thick lines indicate filling of edge states as dictated by k_2 , chosen to illustrate system thermalized at k_2^i and then carried adiabatically to k_2^f . Inset: edge states associated with left (green) and right (blue) surfaces.

between surface charge and bulk polarization assumes that the surface is insulating, with the Fermi level lying in a gap common to both the bulk and surface [9]. When chiral edge states are present, the surfaces cannot be insulating, so the usual conditions are violated.

To show how Eq. (7) can be corrected for the case of a CI, let us again consider our Haldane model ribbon at some fixed k_2 . Its surface charge can be calculated from $P_1 = P \hat{b}_1 = (S/a_2)P_1$ with P_1 evaluated using Eq. (9), but its value will depend on the choice of the k_2 at which the occupation of the edge state has its discontinuity, so that

$$P_1^{[k_2]} = \frac{e}{N_1 a_2} \sum_{n \in N} \int_0^{2\pi} dk_2 \sum_{j_1, j_2} \langle \hat{r}_1 \rangle_{n k_2, j_1; n k_2, j_2}; \quad (10)$$

where N is the set of N_1 occupied states at k_2 given the specified k_2 (i.e., the choice whether the L or R edge state is included in N as k_2 passes through k_2^*).

Since the surface charge theorem of Eq. (7) for ordinary insulators was demonstrated via the Wannier representation [9], we take the same approach here. However, well-localized bulk WFs do not exist in a CI [4], so we focus instead on "hybrid Wannier functions" (HWFs) [13] in which the Fourier transform from Bloch functions is carried out in the r_1 direction only. Thus k_2 remains a good quantum number and the HWF

$$W_{k_2}(r_1; r_2) = \frac{1}{N_1} \sum_{k_1} \int_0^{2\pi} dk_1 \psi_{k_1 k_2}(r_1; r_2) \quad (11)$$

is well localized only in the a_1 direction. Using these we can represent the polarization

$$P_1^{[k_2]} = \frac{e}{S} \sum_{j_2} \int_0^{2\pi} dk_2 \langle \hat{r}_1 \rangle_{k_2, j_2} \quad (12)$$

in terms of the HWF center $[\gamma_2]_{k_2} = \frac{1}{N_1} \sum_{n=1}^{N_1} \langle \psi_{k_2} | \hat{r}_1 | \psi_{k_2} \rangle$. We require $[\gamma_2]_{k_2}$ to be a continuous function of $k_2 \in [k_2^*, k_2^* + 1]$ so as to guarantee a result that is equivalent to Eqs. (1-3).

To make the connection between Eqs. (10) and (12), we recast the former by constructing Wannier-like functions along the a_1 direction for the finite-width strip, starting from the $N_1 \times N_1$ matrix $R_{m,n;k_2}^{[\gamma_2]} = \langle \psi_{k_2} | \hat{r}_1 | \psi_{k_2} \rangle$, where $m, n \in [1, N_1]$ as specified by k_2 . The N_1 eigenvectors of $R_{k_2}^{[\gamma_2]}$ correspond to states that are Bloch-like along r_2 but localized along r_1 , which we refer to as ribbon HWFs, and the eigenvalues $[\gamma_{jk_2}^{[\gamma_2]}]$ locate their centers of charge. Using the basis-independence of the trace, Eq. (10) can now be rewritten as

$$[\gamma_2] = \frac{e}{N_1 a_2} \sum_{j=1}^{N_1} \int_{k_2^*}^{k_2^*+1} dk_2 [\gamma_{jk_2}^{[\gamma_2]}] \quad (13)$$

The similarity between Eqs. (12) and (13) suggests that these can be connected. Since k_2 is a good quantum number, each k_2 can be treated independently. For each k_2 we can compare the infinite (bulk) 1D system described by Eq. (12) with the finite (ribbon) 1D system described by Eq. (13). The essential observation is that, in the limit of large N_1 , the HWF centers $[\gamma_{jk_2}^{[\gamma_2]}]$ deep inside the ribbon converge to the bulk $[\gamma_{k_2}^{[\gamma_2]}]$, modulo an integer [9]. This is illustrated in Fig. (3), where both sets of HWF centers are plotted as a function of k_2 for a ribbon of width $N_1 = 6$. Furthermore, the fact that the occupation of edge states switches between L and R edge at k_2 is reflected in the discontinuity of ribbon HWF centers $[\gamma_{jk_2}^{[\gamma_2]}]$ at k_2 . On the other hand, the bulk HWF centers $[\gamma_{k_2}^{[\gamma_2]}]$ are chosen to be continuous across k_2 . We can account for this discrepancy either by including a correction term proportional to $(k_2 - k_2^*)$,

$$[\gamma_2] = \frac{1}{a_2} \sum_{j=1}^{N_1} \left(\frac{1}{2} [\gamma_{jk_2}^{[\gamma_2]}] + eC(k_2 - k_2^*) \right) \pmod{e=a_2}; \quad (14)$$

or by realizing that by the virtue of Eq. (5) this is equivalent to shifting the reciprocal space origin to k_2 ,

$$[\gamma_2] = \frac{S}{a_2} P_1 [\gamma_2] \pmod{e=a_2}; \quad (15)$$

as can be seen from the dashed frame in Fig. 3. Eq. (14) or (15) is the appropriate generalization of the surface charge theorem, Eq. (7), to the case of a CI, and should be correct in large N_1 limit for both thermally and adiabatic fillings as long as the appropriate k_2^* is used.

We have also tested the correctness of this formula using our numerical calculations on the modified Haldane model. Recall that the solid curve in Fig. 1(b) represents the surface charge as computed from Eq. (9) for the thermalized case. For each μ , we first locate k_2 using 1000 k-points on a ribbon of width $N_1 = 70$ and evaluate Eq. (15) with $k_2 = k_2^*$ using Eqs. (2-3) on a 250×250 k-point mesh. The resulting values are plotted as blue dots in Fig. 1(b). The agreement is excellent.

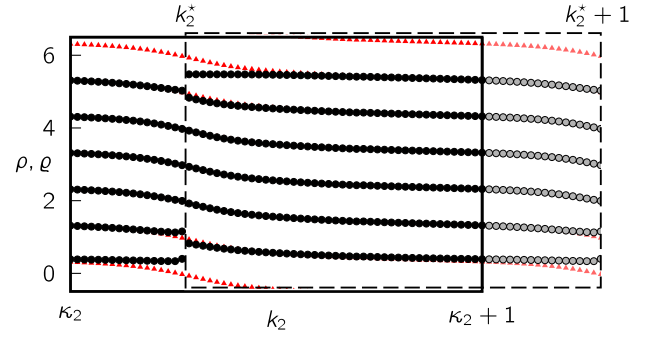


FIG. 3: (Color online) Black dots show ribbon HWF centers $[\gamma_{jk_2}^{[\gamma_2]}]$ and red triangles bulk HWF centers $[\gamma_{k_2}^{[\gamma_2]}]$ and its periodic images as a function of k_2 . Dashed frame corresponds to choice of origin at discontinuity in $[\gamma_{jk_2}^{[\gamma_2]}]$, k_2 .

In summary, we have generalized the Berry-phase concept of polarization to the case of a Chern insulator. The integrated current flow during adiabatic evolution is given by Eq. (6), where the reciprocal-space cell must be the same in both terms on the right-hand side. The surface charge at an edge of a bounded sample is given by Eq. (15), where k_2 specifies the wavevector at which the occupation discontinuity occurs in the chiral edge state. These results may be of use in understanding the physical properties of these topological insulators, and perhaps in searching for experimental realizations.

We acknowledge useful discussions with P. Chandra. This work was supported by NSF Grant DMR-0549198.

Electronic address: sinisa@physics.rutgers.edu

- [1] F. D. M. Haldane, Phys. Rev. Lett. 61, 2015 (1988).
- [2] D. J. Thouless, Topological Quantum Numbers in Non-relativistic Physics (World Scientific, Singapore, 1998).
- [3] D. J. Thouless, M. Kohmoto, M. P. Nightingale, and M. den Nijs, Phys. Rev. Lett. 49, 405 (1982).
- [4] C. Brouder, G. Panati, M. Calandra, C. Mourougane, and N. Marzari, Phys. Rev. Lett. 98, 046402 (2007).
- [5] T. Thonhauser and D. Vanderbilt, Phys. Rev. B 74, 235111 (2006).
- [6] R. Resta and S. Sorella, Phys. Rev. Lett. 82, 370 (1999).
- [7] N. Marzari and D. Vanderbilt, Phys. Rev. B 56, 12847 (1997).
- [8] R. D. King-Smith and D. Vanderbilt, Phys. Rev. B 47, 1651 (1993).
- [9] D. Vanderbilt and R. D. King-Smith, Phys. Rev. B 48, 4442 (1993).
- [10] R. Resta and D. Vanderbilt, in Modern Ferroelectrics, edited by C. Ahn and K. Rabe (Springer-Verlag, Berlin, 2007), pp. 31-68.
- [11] I. Souza, T. Wilkens, and R. M. Martin, Phys. Rev. B 62, 1666 (2000).
- [12] Note that $P_1 \neq 0$ even for $\mu = 0$, since $\mu \neq 0$ allows for an asymmetric population of the edge states.
- [13] C. Sgieravello, M. Peressi, and R. Resta, Phys. Rev. B 64, 115202 (2001).